# Lattice dynamics and the high-pressure equation of state of Au

Carl W. Greeff and Matthias J. Graf
*Los Alamos National Laboratory, Los Alamos, New Mexico 87545, USA*
(Received 26 August 2003; published 19 February 2004)

Elastic constants and zone-boundary phonon frequencies of gold are calculated by total energy electronic structure methods to twofold compression. A generalized force constant model is used to interpolate throughout the Brillouin zone and evaluate moments of the phonon distribution. The moments are used to calculate the volume dependence of the Grüneisen parameter in the fcc solid. Using these results with ultrasonic and shock data, we formulate the complete free energy for solid Au. This free energy is given as a set of closed-form expressions, which are valid to compressions of at least $V/V_0=0.65$ and temperatures up to melting. Beyond this density, the Hugoniot enters the solid-liquid mixed phase region. Effects of shock melting on the Hugoniot are discussed within an approximate model. We compare with proposed standards for the equation of state to pressures of $\sim$200 GPa. Our result for the room-temperature isotherm is in very good agreement with an earlier standard of Heinz and Jeanloz.

DOI: 10.1103/PhysRevB.69.054107 PACS number(s): 62.50.+p

## I. INTRODUCTION

The elastic constants, phonon frequencies, and equation of state (EOS) are fundamental properties of matter. The values of these parameters under compression find application in geophysics[1] and in the prediction and interpretation of processes of dynamic compression.[2,3] For many materials, especially elemental metals, the principal Hugoniot curves, the set of states accessible via a single shock from ambient conditions, have been measured.[2,4–6] Since the pressure, density, and internal energy are known along the Hugoniot from the jump conditions,[2] these data are an important baseline for high-pressure equations of state. The off-Hugoniot EOS is needed for the prediction of processes involving more complicated loading paths, such as multiple shocks or shock and release.[7] Extrapolation from the Hugoniot has also been used to establish pressure standards for static high-pressure experiments, whose room-temperature isotherms are regarded as known.[2,8,9] Au has been used as a standard in this way, and has been used to calibrate the ruby $R_1$ line as a secondary standard.[9–11] Recent studies have called into question the accuracy of the gold pressure standard. Akahama *et al.*[12] compressed Au and Pt in the same cell and found two Au standards[8,13] to give pressures lower than Pt by 20 and 15 GPA, respectively, at 150 GPa. Shim *et al.*,[14] on the other hand, propose a new EOS for Au that gives pressures still lower than either of these earlier standards.

To relate the Hugoniot to the room-temperature isotherm requires information on the Grüneisen parameter $\gamma = V(\partial P/\partial E)_V$ and the specific heat $C_V$.[2] These are dominated by lattice vibrations in the regimes under consideration here. With increasing compression, the separation between the Hugoniot pressure and the room-temperature pressure increases, resulting in greater dependence of the inferred room-temperature isotherm on $\gamma$. Because $\gamma$ is not easily measured at high pressure, this introduces a non-negligible source of uncertainty in the pressure standards. In most cases, a model assumption of the form $\gamma(V)=\gamma(V_0)(V/V_0)^q$ has been used. The specific value $q=1$ has been used often in shock work.[2,8] However, a power-law dependence of $\gamma$ on $V$ is qualitatively incorrect at high compression, and extrapolation on this basis is inherently limited.

In principle, the various components of the EOS—the static lattice energy, the vibrational free energy, and the electronic excitation free energy—can be evaluated from electronic structure theory. Practical calculations based on approximate density-functional theories typically have errors of several percent in the density at zero pressure and 10% or more in the bulk modulus.[15] These are unacceptably large errors for the purpose of high accuracy equations of state. These properties can be measured accurately, and are mainly determined by the cold energy curve, which is the largest contribution to the EOS in the regime considered here. On the other hand, we find that *ab initio* electronic structure calculations are capable of obtaining phonon frequencies of sufficient accuracy to strongly constrain the volume dependence of the Grüneisen parameter $\gamma$. We therefore propose that the most accurate EOS in the solid is obtained by combining an empirical cold energy with *ab initio* lattice vibration and electronic excitation free energies. This is analogous to procedures that have been used to reduce shock Hugoniot data and derive room-temperature standards, but the present analysis gives a strong physical foundation for the volume dependence of $\gamma$, allowing confidence in the results at higher compression. We are not aware of any evidence of solid-solid phase transitions in Au, and we consider only the fcc solid. Recent calculations[16] indicate a transition to the hcp structure for $V/V_0 \lesssim 0.6$, and we do not attempt to extend our solid EOS beyond this density.

This paper is arranged as follows. First we discuss lattice dynamics and its connection to the EOS. We emphasize the importance of the classical limit for defining the ion motion contribution to $\gamma$. We describe our procedures for calculating phonon frequencies and interpolating to the whole Brillouin zone. Next we present our results for elastic and phonon properties of Au, and our analysis to obtain $\gamma^{\mathrm{ion}}(V)$. We then present the complete EOS for solid Au by giving a set of closed-form expressions for the Helmholtz free energy with parameters. The resulting room-temperature isotherm is compared with various proposed standards. Next we discuss

 

shock melting and its effect on the Hugoniot within an approximate model, and finally give our conclusions.

## II. LATTICE DYNAMICS AND THE EQUATION OF STATE

We write the Helmholtz free energy as

$$F(V,T)=\phi_0(V)+F^{\mathrm{ion}}(V,T)+F^{\mathrm{el}}(V,T), \tag{1}$$

where $\phi_0$ is the static lattice energy, $F^{\mathrm{ion}}$ is the ion motion free energy, and $F^{\mathrm{el}}$ is the electronic excitation free energy. In our applications, $\phi_0$ gives the largest contribution to the pressure. The ion motion free energy gives the dominant temperature dependence of $P=-(\partial F/\partial V)_T$. The electronic excitation term $F^{\mathrm{el}}$ is generally a small correction to the solid EOS, becoming important for the liquid Hugoniot at several hundred gigapascals.

It is, therefore, imperative to have an accurate $F^{\mathrm{ion}}$ for calculating the temperature dependence of $P$. The quasiharmonic approximation has been found to have small errors in many cases.[17] We have carried out Monte Carlo simulations using an embedded atom model[18] of Cu to investigate the importance of anharmonic corrections to the ion free energy. Here we define the anharmonic free energy to be the difference between the true ion free energy and the quasiharmonic approximation, noting that the term has been used differently[19] by other authors.[20] We intend to publish details of our Cu simulations elsewhere. In summary, we find that up to 300 GPa on the melting curve, $|P^{\mathrm{anh}}|<0.85$ GPa, and is never more than 3% of the *thermal* pressure $P(V,T)-P(V,0)$, a very small correction to the total pressure. Given the similarity of the bonding in Cu and Au, we expect these results to be relevant for Au also. Thus, in what follows we neglect anharmonicity and use the quasiharmonic approximation for $F^{\mathrm{ion}}$,

$$F^{\mathrm{ion}}(V,T)=3N\int_0^\infty d\omega g(\omega)[\tfrac{1}{2}\hbar\omega+k_BT\ln(1-e^{-\hbar\omega/k_BT})], \tag{2}$$

where we have introduced $g(\omega)=(1/3N)\Sigma_{\mathbf{k}}\delta(\omega-\omega_{\mathbf{k}})$, the normalized phonon density of states. The phonon frequencies $\omega_{\mathbf{k}}$ are functions of volume only, and the sum is over the $3N$ normal modes of the crystal.

Application of Eq. (2) requires the full phonon density of states $g(\omega)$ at all volumes. While in principle this information is available from our calculations, in practice the classical limit dominates our EOS, allowing for a substantial simplification. In the classical limit, which is the leading term in the high-temperature expansion of Eq. (2), the free energy is given by

$$F^{\mathrm{cl}}(V,T)=3Nk_BT\ln\left(\frac{e^{-1/3}\hbar\omega_0}{k_BT}\right), \tag{3}$$

where we have introduced the moment

$$\omega_0=e^{1/3}\exp\left[\int_0^\infty d\omega\, g(\omega)\ln\omega\right]. \tag{4}$$

Other moments are conventionally defined as

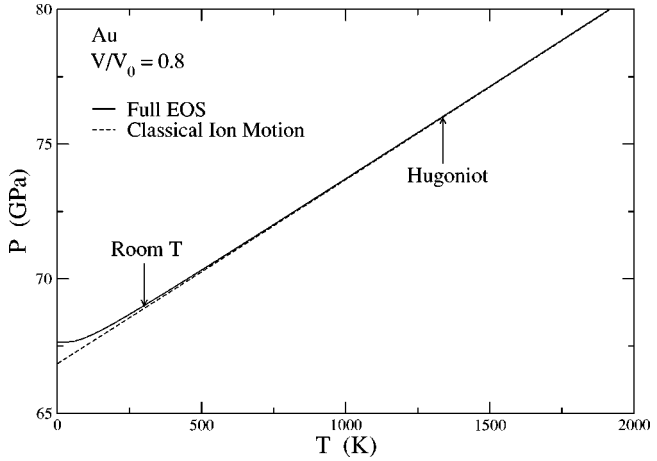


FIG. 1. Role of quantum ion motion in the EOS. Graph shows $P(T)$ along an isochore $V/V_0=0.8$. Solid curve is the full EOS and dashed curve uses the classical limit of the ion free energy. Hugoniot temperature at the given density is 1340 K.

$$\omega_n=\left[\frac{3+n}{3}\int_0^\infty d\omega\, g(\omega)\omega^n\right]^{1/n}, \quad n\neq 0, \quad n>-3, \tag{5}$$

where the normalizations in Eqs. (4) and (5) are chosen so that for a Debye spectrum, described by

$$g(\omega)=\frac{3}{\omega_D^3}\omega^2\Theta(\omega_D-\omega), \tag{6}$$

all $\omega_n$ are equal to $\omega_D$, the Debye frequency. We subsequently give results for $\nu_n=\omega_n/(2\pi)$ corresponding to the experimental convention of giving frequencies $\nu$ in Hertz, as opposed to angular frequencies $\omega$.

In the classical limit, the ion pressure is linear in $T$ with $(\partial P^{\mathrm{ion}}/\partial T)_V=(3Nk_B/V)\gamma_0$, where $\gamma_0=-d\ln\omega_0/d\ln V$, and the specific heat is constant, $C_V=3Nk_B$. The role of quantum ion motion in the EOS is illustrated in Fig. 1, which shows the pressure along an isochore $V/V_0=0.8$. The solid curve is our full EOS, described below, and the dashed curve uses the classical limit of $F^{\mathrm{ion}}$ at all $T$. The arrows mark room temperature and the Hugoniot temperature, which is 1340 K at the given density. The melting temperature at this density is estimated to be 4900 K, beyond the range of the plot. It is clear that the classical limit dominates even at room temperature. The Hugoniot is well into the classical regime. At higher densities, the Hugoniot is still further above the quantum regime. The largest quantum effect on the pressure is at $T=0$, where the zero-point vibrations contribute a pressure of 0.8 GPa at this density. The classical limit is clearly dominant for interpolating between the Hugoniot and room temperatures.

We have found that an interpolation based on the Debye model gives a very accurate approximation to the full quasiharmonic free energy. The Debye free energy is a special case of the quasiharmonic free energy, Eq. (2). Inserting the Debye density of states, Eq. (6), gives

$$F^{\mathrm{D}}(V,T)=N[\tfrac{9}{8}\hbar\omega_D+3k_BT\ln(1-e^{-\hbar\omega_D/k_BT}) - k_BTD(\hbar\omega_D/k_BT)], \quad (7)$$

where

$$D(x)=\frac{3}{x^3}\int_0^x dz\,\frac{z^3}{e^z-1}. \quad (8)$$

In light of the above remarks, it is important to capture the correct classical limit. This requires that we set

$$\omega_D(V)=\omega_0(V). \quad (9)$$

To emphasize the distinction between Eq. (9) and the standard definition of $\omega_D$ in terms of acoustic velocities, we refer to the Debye free energy together with Eq. (9) as the high-temperature Debye model. The high-temperature Debye model gives the same results as the full quasiharmonic free energy in the classical regime, and in addition obeys the Nernst theorem at low $T$. We have checked that at low $T$, the error in the pressure compared to the full quasiharmonic approximation is entirely negligible.

Thus, we can simplify the specification of the lattice vibration free energy from giving $g(\omega)$ at all $V$ to giving the single moment $\omega_0$ at all $V$. This is advantageous for numerical applications. It also allows us to express our full EOS in a few compact formulas so that it is generally accessible. These formulas are given below.

Calculating the moments $\omega_n$ requires the phonon frequencies for all $\mathbf{k}$ in the Brillouin[21,22] zone. Direct *ab initio* calculations on a dense mesh in $\mathbf{k}$ would be quite expensive. As a result of another study[23] we found that the low-order moments can often be accurately obtained from short-ranged force-constant models. In particular, for Au, the moment $\omega_0$ is converged to less than 1% with a second nearest neighbor (2NN) model. Therefore, our method is to calculate four zone-boundary phonon frequencies corresponding to the transverse and longitudinal modes at the $X$ and $L$ points. These are calculated with standard frozen-phonon methods. In addition the three elastic moduli are calculated using the method described by Söderlind *et al.*[24] We fit these results to a 2NN force-constant model, which then allows the evaluation of $\omega_{\mathbf{k}}$ for arbitrary $\mathbf{k}$ for integration over the Brillouin zone.

The electronic structure calculations used the full-potential linearized augmented plane-wave code WIEN97.[25] We used the local-density approximation (LDA) rather than the generalized gradient approximation (GGA), based on Boettger's finding[16] that the LDA gives a better static lattice energy than the GGA for Au. Some numerical parameters used in the calculations were, in atomic units, the following: muffin tin radius $r_{\mathrm{MT}}=2.0$, plane wave cutoff $r_{\mathrm{MT}}k_{\max}=9.0$, cutoff for expansion of density and potential $g_{\max}=14$. For elastic modulus calculations, Brillouin-zone integrals used special points corresponding to $18^3$ points in the full zone, with Gaussian smearing of the energies by 20 mRy. The zone-boundary phonons were found to be comparatively insensitive to the $\mathbf{k}$-point mesh, and smaller meshes of $10^3$ points were used. The $5p$, $5d$, and $6s$ shells were treated as valence states, and local orbital extensions[26] were used in the $p$ and $d$ channels.

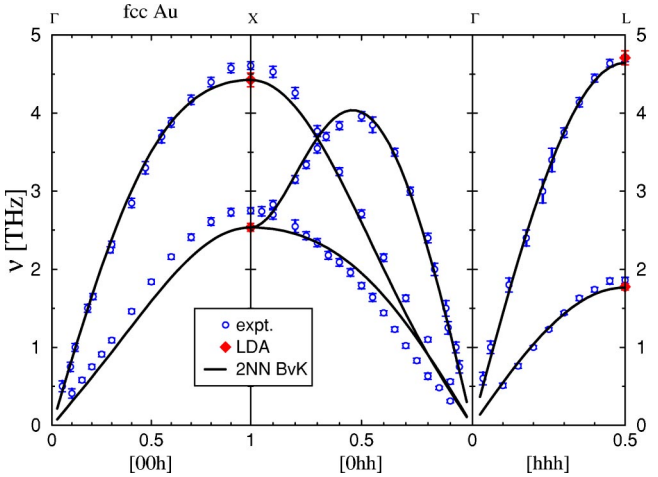


FIG. 2. (Color online) Phonon dispersion for Au at room temperature and ambient pressure. Open circles are experimental data of Lynn *et al.* (Ref. 27). Filled diamonds are LDA calculations of zone-boundary phonons at the $X$ and $L$ points. Solid curve is interpolation based on fit of 2NN force constant model to the LDA zone-boundary phonons and elastic moduli.

We used a generalized Born-von Kármán force model for our lattice-dynamical calculations, from which we were able to compute the phonon dispersions in the entire Brillouin zone. Since gold has a very simple phonon dispersion, we employed only a model with 1NN and 2NN interatomic shells of atoms. In fcc lattice the 1NN and 2NN forces are determined by three and two independent parameters, respectively (for more details see, e.g., Ref. 23). These five force constants were extracted by fitting simultaneously the phonon frequencies of gold at the $X$ and $L$ points of the Brillouin zone and the elastic constants $C_{11}$, $C_{12}$, and $C_{44}$ near the zone center ($\Gamma$ point). Thus we fit a total of seven independent data points. We gave equal weight to the zone-boundary phonons and elastic constants in our $\chi^2$ fit of the phonon dispersions. Although the 2NN Born-von Kármán force model is too simple to reproduce all phonon frequencies within less than approximately 10%, see Fig. 2, it is sufficiently accurate to compute integrated quantities such as the phonon moments within less than approximately 3%. More accurate phonon dispersions can be obtained if needed, by computing *ab initio* frequencies at half and quarter distances in the Brillouin zone and fitting those to a 3NN or higher-order Born-von Kármán force model, or to phonon models with interatomic pseudopotentials.

## III. ELASTIC AND PHONON PROPERTIES

Figure 2 shows the calculated phonon dispersion curves for Au at the density corresponding to ambient pressure and room-temperature. The filled diamonds at the $X$ and $L$ points are the LDA frozen phonon results. These together with the calculated elastic moduli are used to obtain the force constants. The solid curves are the interpolation to general wave

TABLE I. Calculated phonon and elastic properties of Au. $V_0$ is the volume at 298 K and atmospheric pressure and is 10.212 $cm^3$/mol for Au. Frequencies $\nu$ given in terahertz and elastic moduli given in gigapascal.

| $V/V_0$ | $\nu_{Xt}$ | $\nu_{Xl}$ | $\nu_{Lt}$ | $\nu_{Ll}$ | $C'$ | $C_{44}$ | $B$ | $\nu_0$ | $\nu_1$ | $\nu_2$ |
|---|---|---|---|---|---|---|---|---|---|---|
| 1.1 | 1.76 | 3.17 | 1.33 | 3.37 | 9.2 | 11.1 | 91.0 | 2.53 | 2.60 | 2.68 |
| 1.0 | 2.54 | 4.43 | 1.77 | 4.71 | 13.8 | 27.4 | 172.0 | 3.53 | 3.64 | 3.75 |
| 1.0/expt. | 2.75 | 4.61 | 1.86 | 4.70 | 14.6 | 41.5 | 167. | 3.65 | 3.75 | 3.86 |
| 0.9 | 3.45 | 5.91 | 2.30 | 6.32 | 20.3 | 55.0 | 304.4 | 4.71 | 4.86 | 5.00 |
| 0.8 | 4.55 | 7.71 | 2.95 | 8.40 | 26.8 | 112.3 | 527.3 | 6.16 | 6.35 | 6.54 |
| 0.7 | 5.94 | 10.05 | 3.76 | 11.19 | 37.4 | 221.7 | 928.3 | 8.03 | 8.30 | 8.57 |
| 0.6 | 7.76 | 13.18 | 4.78 | 15.23 | 67.0 | 443.5 | 1663.8 | 10.55 | 10.93 | 11.30 |
| 0.5 | 10.27 | 17.63 | 6.10 | 21.62 | 135.4 | 871.0 | 3097.4 | 13.99 | 14.58 | 15.13 |

vectors using the force-constant model. The open circles are the experimental data of Lynn *et al.*[27] The force-constant model is overconstrained, so it neither goes precisely through the calculated zone-boundary frequencies nor has it exactly the calculated elastic moduli. The shapes of the dispersion curves are simple enough for Au that they are generally well captured by the 2NN model.

Table I summarizes our results for the zone-boundary phonons, elastic moduli, and moments $\nu_n = \omega_n/2\pi$, as functions of volume. The reference volume $V_0$ corresponds to $T = 298$ K and $P = 1$ bar $= 100$ kPa. For Au, $V_0 = 10.212$ $cm^3$/mol or $114.43a_0^3$/atom. Also shown are the experimental data at room temperature.[27,28] No attempt is made to account for the temperature dependence beyond comparing at the correct volume. There is generally good agreement between the calculated and experimental quantities. The main exception is $C_{44}$, which is calculated substantially lower than measured. Our calculation is in better agreement with an earlier LDA calculation.[24] The main result of the present calculation is the value of $\nu_0$, which is within 3% of the measurement. The ratio $\nu_1/\nu_0$ is 1 for a Debye spectrum. Our calculations give $\nu_1/\nu_0 = 1.03$ at ambient density and 1.04 at twofold compression, so, by this measure, the departure from a Debye spectrum is small and nearly constant with volume.

Measurements of elastic moduli were reported by Duffy *et al.*[29] to $P = 37$ GPa, and *ab initio* calculations by Tsuchiya and Kawamura[30] to 100 GPa. Figure 3 shows these results along with our calculations. Our volumes are converted to room-temperature pressures using the EOS described below. The highest density in Table I corresponds to $P \approx 780$ GPa, and the graph is restricted to lower pressures to highlight the comparison with these other works. Our calculations of $C_{11}$ and $C_{12}$ are in good agreement with Tsuchiya and Kawamura, while our $C_{44}$ is systematically lower, in somewhat better agreement with the experiments. Our $C_{11}$ is in good agreement with the experiments while $C_{12}$ is slightly high. It should be noted that the experimental $C_{ij}$ depend on a model parameter $\alpha$ used in the analysis.[29] The plotted points correspond to $\alpha = 1$. It is encouraging that our calculations give the correct trends for the pressure dependence of $C_{ij}$.

Having determined the moments $\nu_n$ as functions of volume, we need to interpolate and differentiate them to obtain thermodynamic functions. To do this, we assumed the following functional form for $\gamma_n(V)$, which has been used in creating many wide ranging equations of state:[31]

$$\gamma_n(V) = \gamma^\infty + A_n\left(\frac{V}{V_0}\right) + B_n\left(\frac{V}{V_0}\right)^2, \tag{10}$$

where $\gamma^\infty$ is the infinite density limit of $\gamma$, and $A_n$ and $B_n$ are parameters. Alternatively, we can express $A_n$ and $B_n$ in terms of $q_n = d\ln(\gamma_n)/d\ln(V)$ and $\gamma_n(V_0)$ as

$$A_n = \gamma_n(V_0)[2 - q_n(V_0)] - 2\gamma^\infty,$$

$$B_n = \gamma_n(V_0)[q_n(V_0) - 1] + \gamma^\infty. \tag{11}$$

Integrating $\gamma_n = -d\ln\nu_n/d\ln V$, we have

$$\nu_n(V) = \nu_n(V_0)\left(\frac{V}{V_0}\right)^{-\gamma^\infty} \exp\left\{-A_n\left[\left(\frac{V}{V_0}\right) - 1\right] - \frac{B_n}{2}\left[\left(\frac{V}{V_0}\right)^2 - 1\right]\right\}. \tag{12}$$

By fitting this functional form to the calculated $\nu_0(V)$, we extract the parameters giving $\gamma_0(V)$. In our fits, we keep $\gamma^\infty$

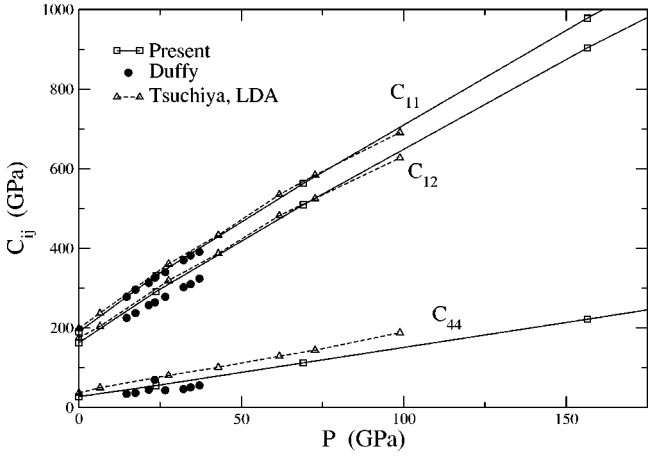


FIG. 3. Pressure dependence of the elastic moduli of Au. Open squares are present LDA calculations with pressures from our EOS. Solid circles are experimental data from Duffy *et al.* (Ref. 29). Open triangles are previous LDA calculations by Tsuchiya and Kawamura.

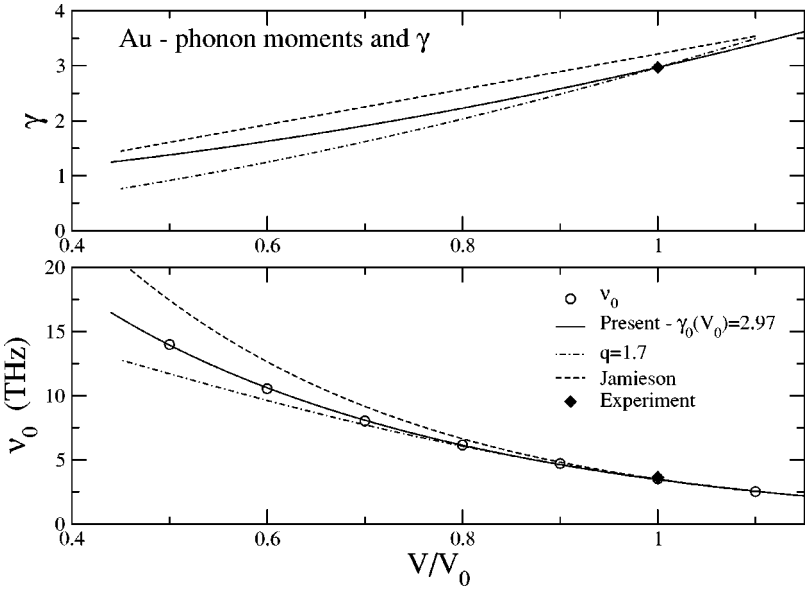


FIG. 4. Volume dependence of $\nu_0$, the log moment of the phonon frequencies, and $\gamma_0 = -d \ln \nu_0 / d \ln V$ for Au. Lower graph is $\nu_0(V)$. Open symbols are calculated moments. Upper graph is resulting $\gamma_0(V)$. Solid curves are present results fitting Eq. (10) to the calculated moments with the constraint $\gamma_0(V_0) = 2.97$. Dash-dot curve shows the commonly used approximation $\gamma(V) = \gamma(V_0)(V/V_0)^q$ for $q = 1.7$ (Ref. 13). Dashed curve corresponds to the $\gamma$ of Jamieson *et al.* (Ref. 8), who used $q = 1$ and $\gamma(V_0) = 3.215$.

fixed. The value $\gamma^\infty = 2/3$ has been widely used,[32] although arguments have been made for $\gamma^\infty = 1/2$.[33] For our application and density range, we have found that the quality of the fit and the resulting $\gamma_0(V)$ are insensitive to this choice, and we use $\gamma^\infty = 2/3$. The fitting procedure is illustrated in Fig. 4, where we show the fit for $\nu_0(V)$, the log moment and the resulting $\gamma_0(V)$. We did the fits with $\nu_0(V_0)$, $\gamma_0(V_0)$, and $q_0(V_0)$ as free parameters, and with $\gamma_0(V_0)$ constrained to the experimental value of 2.97. (This experimental value was determined so that the thermal expansion for the subsequent EOS overlies the recommended curve of Touloukian[34] from 100 to 1200 K.) The unconstrained fit gives $\gamma_0(V_0) = 2.88$. Constraining $\gamma_0(V_0)$ increases the rms error of the fit from $4.9 \times 10^{-2}$ to $5.7 \times 10^{-2}$ THz, which is not a significant increase. Also, we note that constraining $\gamma_0(V_0)$ does not change $\gamma_0(V)$ at smaller $V$. For this reason, we believe that the constrained fit is the best overall approximation for $\gamma^{\rm ion}(V)$ up to twofold compression. This is shown as the solid curve in Fig. 4. The corresponding parameters are $\nu_0(V_0) = 3.46$ THz, $\gamma_0(V_0) = 2.97$, and $q_0(V_0) = 1.37$. We do not show the unconstrained fit in Fig. 4 because it is too close to the constrained fit. The dot-dashed curves correspond to $q = \text{const}$, $\gamma(V) = \gamma(V_0)(V/V_0)^q$. The value $q = 1$ gives a $\gamma$ that is too high over this density range, while $q = 1.7$[13] is too low. Jamieson *et al.*[8] used $q = 1$ and an ambient value $\gamma(V_0) = 3.215$, which results in the dashed curve. We believe that their $\gamma$ is too high at all volumes considered here. Any constant value of $q$ will lead to a $\gamma$ that is too small at very high compression.

## IV. EQUATION OF STATE

The complete EOS is determined when the Helmholtz free energy $F$ is given as a function of volume and temperature. In this section we describe our form for $F$ and give the numerical parameters for fcc Au. First we write the free energy as in Eq. (1) as the sum of the static lattice energy $\phi_0$, an ion motion free energy $F^{\rm ion}$, and an electronic excitation term $F^{\rm el}$. For the ion motion free energy we use the quasiharmonic approximation, and further specialize to the high-temperature Debye model. Thus we take the ion free energy to be given by Eqs. (7) and (8), where we identify $\omega_D$ with the log moment $\omega_0$ of the phonon frequencies. As discussed in Sec. II, this gives the correct classical limit, and leads to extremely small errors at low $T$ compared to the full phonon spectrum. This way we are able to give a closed-form expression for $F^{\rm ion}$, which is very convenient in numerical applications. The volume dependence of $\omega_0$ is that given in Eq. (12) with parameters given above. For the final EOS we have replaced the fitted value of $\omega_0(V_0)$ with the experimental one. This is essentially a small shift in the absolute entropy, which has negligible effect on the results.

Electronic excitations give a small contribution to the thermodynamics, which we approximate by

$$F^{\rm el}(V,T) = -\tfrac{1}{2} N \Gamma(V) T^2. \tag{13}$$

The Sommerfeld coefficient $\Gamma$ is proportional to the electronic density of states at the Fermi energy, $\Gamma = (\pi^2/3) k_B^2 g(\epsilon_f)$. Our calculations show that $d \ln g(\epsilon_f)/d \ln V \approx 0.76$ over the range of densities considered, so we take

$$\Gamma(V) = \Gamma(V_0)(V/V_0)^\kappa \tag{14}$$

with $\kappa = 0.76$. The calculations give $\Gamma(V_0) = 6.7 \times 10^{-4}$ J/mol K$^2$, while the measured value from the low-temperature specific heat is[35] $\Gamma(V_0) = 7.28 \times 10^{-4}$ J/mol K$^2$. The measured low-temperature specific-heat coefficient $\Gamma_{\rm expt}$ is expected to be enhanced with respect to the bare value $\Gamma$ as a result of electron-phonon interactions by a factor $(1+\lambda)$, where $\lambda$ is the dimensionless electron-phonon mass enhancement parameter. The value for gold is $\lambda \approx 0.05$–$0.15$,[36] which agrees with our calculated $\Gamma/\Gamma_{\rm expt} = 1.09$. At high temperatures, $k_B T > \hbar \omega_0$, the phonon mass enhancement becomes ineffective. Hence we use our calculated density of states in the remainder of this paper.

The static lattice energy is needed to complete the free energy. We adopt the functional form due to Vinet *et al.*[37]

$$\phi_0(V) = \frac{4V^*B^*}{(B_1^*-1)^2}[1-(1+X)e^{-X}],$$

$$X = \frac{3}{2}(B_1^*-1)\left[\left(\frac{V}{V^*}\right)^{1/3}-1\right], \quad (15)$$

which is parametrized by the volume at the minimum $V^*$, the bulk modulus $B^*$, and its pressure derivative $B_1^*$. These parameters have been determined empirically by requiring that the EOS reproduce the ambient volume and ultrasonic data for $B_S$ at ambient conditions.[28] For the latter, we adopt the value $B_S = 173$ GPa. Ultrasonic data give values for $(\partial B_S/\partial P)_T$ from 5.2 to 6.4. Therefore, to complete the EOS, we require that it reproduce the measured slope of the Hugoniot, which we take from the fit[4] $U_s = 3.12$ km/s $+ 1.521 U_p$ relating the shock velocity $U_s$ to the particle velocity $U_p$. The resulting parameters give $(\partial B_S/\partial P)_T = 5.49$, consistent with the ultrasonic data.

The complete set of parameters for the free energy of fcc Au is summarized here. The static lattice energy is given by Eq. (15) with

$$V^* = 10.0834 \text{ cm}^3/\text{mol},$$

$$B^* = 180.0 \text{ GPa},$$

$$B_1^* = 5.55. \quad (16)$$

The ion motion free energy is given by Eqs. (7) and (8) with the volume dependence of $\omega_D$ given by Eq. (12) (with $\nu_0 \rightarrow \omega_D$, $\gamma_0 \rightarrow \gamma$, etc.). The parameters $A$ and $B$ are given in terms of $\gamma(V_0)$ and $q(V_0)$ by Eq. (11). The numerical values are

$$V_0 = 10.212 \text{ cm}^3/\text{mol},$$

$$\omega_D(V_0) = 22.9\times 10^{12} \text{ s}^{-1},$$

$$\gamma(V_0) = 2.97,$$

$$q(V_0) = 1.3677,$$

$$\gamma^\infty = 2/3. \quad (17)$$

Finally, the electronic excitation free energy is given by Eqs. (13) and (14) with

$$\Gamma(V_0) = 6.7\times 10^{-4} \text{ J/mol K}^2,$$

$$\kappa = 0.76. \quad (18)$$

The following calculations use these parameters for the free energy of fcc Au. Once the free energy is known, the pressure, internal energy, etc., can be evaluated. We calculate the Hugoniot by fixing a value of the volume and solving for the temperature such that the jump condition, $E-E_0 = \frac{1}{2}(P+P_0)(V_0-V)$, is solved. Here $E_0$, $V_0$, and $P_0$ correspond to the initial state, taken to be ambient temperature and pressure.

Figure 5 shows the Hugoniot and room-temperature isotherm for the present EOS. The solid symbols are the Hugoniot data.[5,6,38] The dashed line corresponds to the linear fit for $U_s(U_p)$. Also shown as the open circles are the room-temperature data from Heinz and Jeanloz[13] taken to 70 GPa with the ruby pressure scale. The open squares are the room-temperature data of Bell *et al.*[11] to 188 GPa. The pressure shown in the graph is taken from the ruby scale, which is extrapolated from a lower-pressure calibration.[9] Our calculations agree with these data to 3% at the highest pressure, indicating support for the extrapolation of the ruby scale.

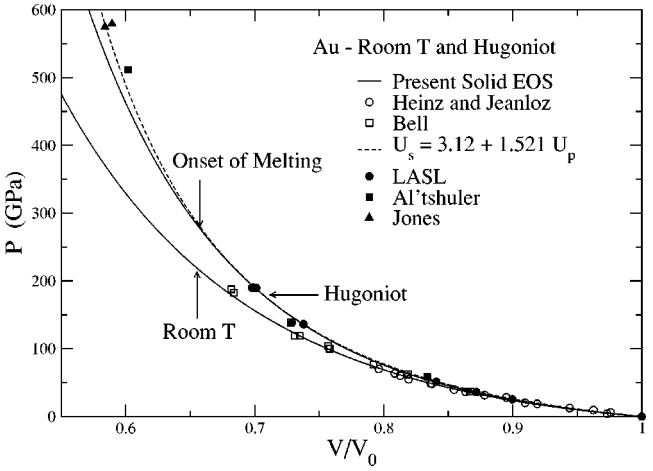


FIG. 5. Hugoniot and room-temperature isotherm of Au. Solid curves are present solid EOS. Solid symbols are Hugoniot data (Refs. 5,6, and 38). Note that there are five overlapping Hugoniot points at $V/V_0 \approx 0.7$. Open symbols are room-temperature data (Refs. 11 and 13). For the Bell *et al.* data (Ref. 11), pressures are from the extrapolated ruby standard. The onset of shock melting is estimated at $P \approx 280$ GPa, as marked.

For $V > 0.656V_0$, the Hugoniot lies in the solid. By matching the measured Hugoniot with our theoretically based Grüneisen parameter, we confirm the accuracy of our room-temperature isotherm, and we have high confidence in our EOS to this density. Combining our calculated Hugoniot temperatures with a Lindemann melting curve, we estimate that the Hugoniot enters a solid-liquid coexistence region at $V/V_0 = 0.656$, $P = 280$ GPa. A more extensive discussion of shock melting is given in the following section. There we find that explicitly accounting for melting leads to good agreement with the high-pressure Hugoniot data, indicating that our solid EOS is valid to densities of $V/V_0 \approx 0.6$.

Figure 6 shows our room-temperature isotherm along with data from Heinz and Jeanloz,[13] and Bell *et al.*[11] Also shown are some of the proposed EOS standards. Jamieson *et al.*[8] used the Hugoniot as a reference, and calculated the room-temperature isotherm using a Mie-Grüneisen EOS. They assumed $\gamma/V = \text{const}$, and used $\gamma(V_0) = 3.215$, so their $\gamma$ is always larger than ours. This results in lower room-temperature pressures than ours, but by restricting their analysis to $V/V_0 > 0.775$, the impact of the assumed $\gamma$ is minimized. The Heinz and Jeanloz EOS is based on extrapolating their room-temperature data, with some consideration of the shock data. Our room-temperature isotherm is in good agreement with Heinz and Jeanloz to 200 GPa. The recently

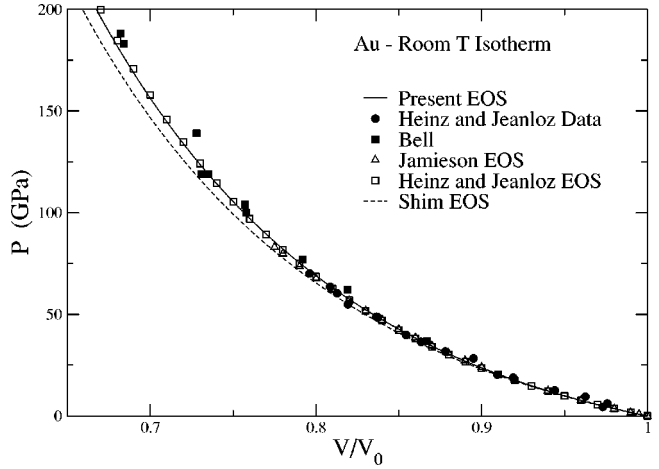


FIG. 6. Room-temperature isotherm of Au. Solid curve is present EOS. Solid symbols are data (Refs. 11 and 13). Open triangles are the EOS of Jamieson *et al.* (Ref. 8). Open squares are EOS of Heinz and Jeanloz (Ref. 13). Dashed curve is EOS of Shim *et al.* (Ref. 14).

proposed EOS of Shim *et al.*[14] is significantly lower than all the other standards. It is lower than the present analysis by 10 GPa at $V/V_0=0.7$, corresponding to $P=156$ GPa.

Figure 7 shows $P(T)$ along two isochores in comparison with various equations of state. At $V/V_0=0.8$, Jamieson *et al.* give somewhat lower $P$ at 300 K with a larger $dP/dT$, in keeping with their higher $\gamma$. Heinz and Jeanloz[13] are in the best overall agreement with the present pressures, with somewhat lower $dP/dT$. Shim *et al.*[14] give a somewhat higher $dP/dT$ with $P$ generally low due to their large offset at room-temperature. Anderson *et al.*[19] adopted the room-temperature isotherm from Heinz and Jeanloz.[13] Their EOS gives $dP/dT$ substantially too low at compressed volumes.

We have tabulated $P(V,T)$ in Table II in the same format adopted by other authors. As discussed, we have extended the range of densities to $V/V_0=0.6$ and the temperatures to 5000 K, except where such temperatures are thought to lie in the liquid phase. Boettger[16] has proposed an extension of the Au 300 K standard to 500 GPa based on LDA calculations. He gives $P=344$ GPa at $V/V_0=0.6$ compared to 329 GPa from our semiempirical EOS. Given the scatter in the high-pressure Hugoniot data, and our approximate treatment of melting, this 4.6% difference is probably within the uncertainties of the present analysis at this high density.

## V. MELTING AND THE HUGONIOT

In order to investigate the effects of melting on the Hugoniot, we have constructed a two-phase model free energy. The ion free energy in the liquid is based on the assumptions that $C_V^{\rm ion}=3Nk_B$, which is reasonable for temperatures near melting, and that $\Delta S_V^{\rm ion}$, the entropy difference between solid and liquid at fixed volume, is $0.8Nk_B$. These are empirically based model assumptions.[39] A statistical mechanical basis for these observations is discussed by Wallace,[40] who argues for the universality of $\Delta S_V^{\rm ion}$. Beyond these assumptions, we require the energy of the liquid with respect to the solid to fully determine the liquid free energy. We do this by imposing that the melting curve, obtained by equating the pressures and Gibbs free energies of liquid and solid, follows the Lindemann rule in the form

$$\frac{T_m}{\omega_0^2(V_s)V_s^{2/3}}=\text{const}, \tag{19}$$

where $V_s$ is the volume on the solidus. The electron excitation free energy is assumed to be the same in the liquid as in the solid. Application of this method to Cu leads to a shock melting threshold of 228 GPa, which compares well with 232 GPa obtained by Hayes *et al.*[41] by analyzing sound speed data. The Au Hugoniot has been calculated for the two-phase model allowing for coexistence in the shocked

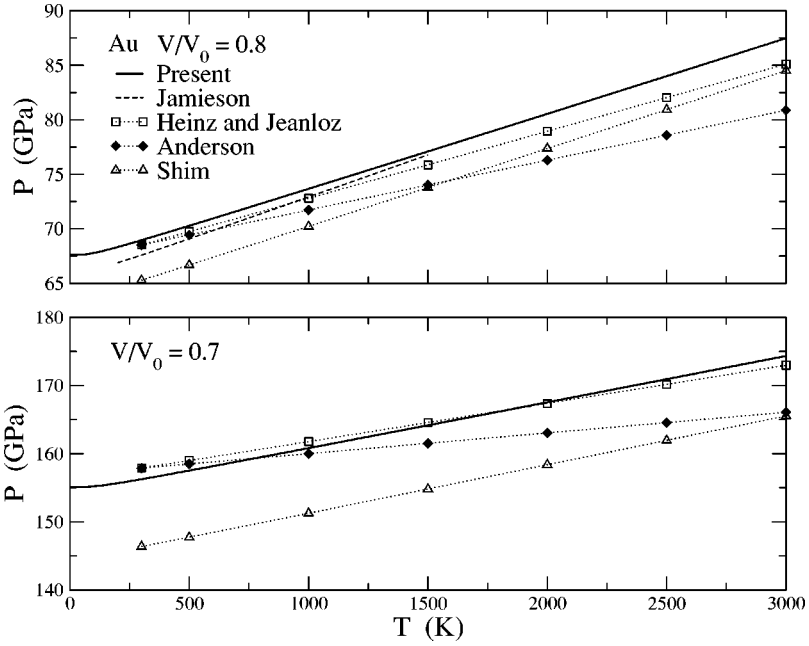


FIG. 7. Isochores of Au. Solid curves are the present EOS. Dashed curve is Jamieson *et al.* (Ref. 8). Open squares are Heinz and Jeanloz (Ref. 13). Filled diamonds are Anderson *et al.* (Ref. 19). Open triangles are Shim *et al.* (Ref. 14).

TABLE II. Tabulated pressures for Au. Compression $\eta = 1 - V/V_{300}$ where $V_{300}$ is the volume at $T = 300$ K and $P = 0$. Pressures in gigapascal. Values in parenthesis are the first liquid states for each $\eta$, included for interpolation. Remaining liquid states left blank.

| $\eta$ | 300 K | 500 K | 1000 K | 1500 K | 2000 K | 2500 K | 3000 K | 3500 K | 4000 K | 4500 K | 5000 K |
|---|---|---|---|---|---|---|---|---|---|---|---|
| 0.00 | 0.00 | 1.44 | 5.08 | 8.73 | (12.40) | | | | | | |
| 0.02 | 3.57 | 5.00 | 8.61 | 12.24 | (15.88) | | | | | | |
| 0.04 | 7.65 | 9.07 | 12.65 | 16.25 | 19.87 | (23.50) | | | | | |
| 0.06 | 12.31 | 13.71 | 17.27 | 20.85 | 24.44 | (28.04) | | | | | |
| 0.08 | 17.61 | 19.01 | 22.53 | 26.09 | 29.66 | 33.24 | (36.83) | | | | |
| 0.10 | 23.65 | 25.03 | 28.54 | 32.07 | 35.61 | 39.17 | 42.74 | (46.33) | | | |
| 0.12 | 30.53 | 31.90 | 35.38 | 38.88 | 42.41 | 45.94 | 49.50 | (53.06) | | | |
| 0.14 | 38.36 | 39.71 | 43.17 | 46.65 | 50.16 | 53.67 | 57.20 | 60.74 | (64.30) | | |
| 0.16 | 47.27 | 48.61 | 52.04 | 55.51 | 58.99 | 62.48 | 65.99 | 69.51 | 73.05 | (76.60) | |
| 0.18 | 57.41 | 58.74 | 62.15 | 65.60 | 69.06 | 72.53 | 76.02 | 79.53 | 83.04 | (86.57) | |
| 0.20 | 68.96 | 70.28 | 73.67 | 77.09 | 80.54 | 83.99 | 87.47 | 90.95 | 94.45 | 97.96 | (101.49) |
| 0.22 | 82.12 | 83.43 | 86.80 | 90.21 | 93.63 | 97.07 | 100.53 | 104.00 | 107.48 | 110.98 | 114.49 |
| 0.24 | 97.13 | 98.43 | 101.78 | 105.17 | 108.58 | 112.00 | 115.44 | 118.90 | 122.37 | 125.85 | 129.34 |
| 0.26 | 114.27 | 115.55 | 118.89 | 122.26 | 125.65 | 129.07 | 132.49 | 135.93 | 139.39 | 142.85 | 146.34 |
| 0.28 | 133.85 | 135.12 | 138.44 | 141.80 | 145.18 | 148.58 | 151.99 | 155.42 | 158.86 | 162.32 | 165.79 |
| 0.30 | 156.25 | 157.51 | 160.81 | 164.16 | 167.53 | 170.92 | 174.32 | 177.74 | 181.17 | 184.62 | 188.08 |
| 0.32 | 181.92 | 183.17 | 186.46 | 189.79 | 193.16 | 196.53 | 199.93 | 203.34 | 206.76 | 210.20 | 213.65 |
| 0.34 | 211.38 | 212.63 | 215.90 | 219.22 | 222.58 | 225.95 | 229.34 | 232.74 | 236.16 | 239.59 | 243.04 |
| 0.36 | 245.26 | 246.49 | 249.75 | 253.07 | 256.42 | 259.79 | 263.17 | 266.57 | 269.99 | 273.41 | 276.86 |
| 0.38 | 284.30 | 285.52 | 288.76 | 292.08 | 295.43 | 298.79 | 302.17 | 305.57 | 308.98 | 312.41 | 315.85 |
| 0.40 | 329.37 | 330.58 | 333.82 | 337.14 | 340.48 | 343.85 | 347.23 | 350.63 | 354.04 | 357.47 | 360.91 |

state.[42] Figure 8 shows the resulting Hugoniot in the pressure-volume plane. Also shown in the figure are the data points and the linear $U_s(U_p)$ fit. The dot-dashed curve is the Hugoniot for the solid only. The boundaries of the coexistence region are visible as kinks on the solid curve at 280 and 350 GPa. Above 350 GPa, the Hugoniot is in pure liquid phase. A similar anomaly is shown for Al in a two-phase calculation by Chisolm *et al.*[43] A significant enhancement of the Hugoniot pressure of Au due to melting was also shown in calculations by Godwal *et al.*,[44] however they predict a much lower shock melting threshold than we do. Just above complete melting, the liquid Hugoniot lies above the solid by 30 GPa. The linear $U_s(U_p)$ curve goes smoothly through the melting region to intersect the liquid data.

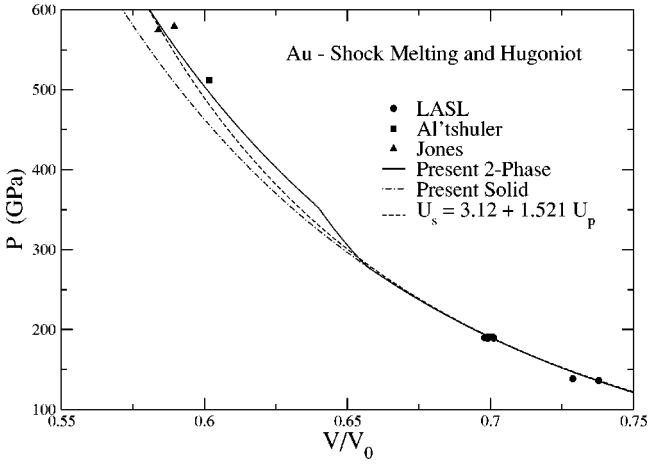


FIG. 8. Hugoniot of Au, including the effects of melting. Solid curve is present two-phase (solid and liquid) EOS. Dot-dashed curve is solid EOS only. Dashed curve is linear fit to $U_s(U_p)$ data (Ref. 4). Solid symbols are measured points (Ref. 5,6, and 38).

Our two-phase EOS gives good agreement with the high-pressure data, which suggests that our cold energy is valid to compressions of $V/V_0 \approx 0.6$. Electronic excitations have practically no effect on the $P(V)$ Hugoniot in the solid phase, although they significantly affect the temperature. At higher temperatures in the liquid, they act to soften the Hugoniot by absorbing energy. Coincidentally, neglecting both electronic excitations and melting gives a Hugoniot that agrees with the linear $U_s(U_p)$ curve quite well to 650 GPa. This is an accidental cancellation of errors. Ignoring melting and electronic excitations gives a temperature that is too high by $\sim 10^4$ K at this pressure. This offsets the neglect of the pressure enhancement due to melting. It is not recommended to ignore either melting or electronic excitations in this high-temperature regime.

## VI. CONCLUSIONS

By combining *ab initio* calculations of elastic moduli and zone-boundary phonons with interpolations based on a force-constant model, we have calculated moments of the phonon frequencies of fcc Au to twofold compression. This allows us to calculate the associated Grüneisen parameters. In particular, we have focused on $\gamma_0$ which corresponds to the classical limit. We emphasize that the classical limit dominates the thermal pressure in the EOS. We find that the frequently used form $\gamma(V) = \gamma(V_0)(V/V_0)^q$ does not represent the volume

dependence of $\gamma$ well. We have used an expansion to second order in $V$ with a physical asymptotic limit, which fits the calculated moments well and is consistent with the measured value of $\gamma$ at ambient pressure and temperature. Using the theoretical $\gamma(V)$ and electron excitation free energy, we have constructed a semiempirical free energy for the solid, which we believe to be as accurate as possible. This free energy is given as a parametrized closed-form expression and the resulting $P(V,T)$ is given in tabular form to $V/V_0=0.6$.

Our static lattice energy is empirical, and is verified by comparison with the measured Hugoniot, so that our EOS can be regarded as a generalization from the Hugoniot with a physically based $\gamma$. In the solid phase, electronic excitations have a small effect. This, together with the dominance of the classical limit in the vibrational free energy, means that the widely used Mie-Grüneisen approximation, that $(\partial P/\partial E)_V$ is independent of $T$, is accurate. At the highest compressions the physics affecting the Hugoniot becomes more complicated. Melting is predicted to begin at 280 GPa and $V/V_0=0.656$. Complete melting is estimated to lead to a 30 GPa increase in the Hugoniot pressure over the solid. At these densities and higher, the Hugoniot temperature is rising rapidly and electronic excitations are playing an increasing role. The highest Hugoniot data are at 580 GPa, where the temperature is calculated to be above $2\times10^4$ K. The Mie-Grüneisen approximation is not expected to be valid for interpolating between the Hugoniot and room temperatures at this high compression, because of the strong effects of melting and electronic excitations. These effects need to be taken explicitly into account, as has been done here.

Regarding EOS standards, our analysis gives a room-temperature $P(V)$ curve that agrees well with that of Heinz and Jeanloz[13] to 200 GPa. Our EOS gives $(\partial P/\partial T)_V$ generally somewhat larger than theirs, and we believe that in this regard our EOS is preferred. The EOS of Jamieson *et al.*[8] is based on reduction of shock data, and was originally given to 80 GPa. It gives somewhat lower pressures than ours, which is due to their use of a Grüneisen parameter that is too large at all volumes. Extrapolation of their room-temperature isotherm to higher pressures[12] is not recommended. Anderson *et al.*[19] adopted the room-temperature isotherm of Heinz and Jeanloz,[13] while giving a different thermal pressure. Their EOS gives $(\partial P/\partial T)_V$ which is substantially too low under compression, and is not recommended for high temperatures. Simultaneous compression of Au and Pt showed[12] that the Pt standard of Holmes *et al.*[45] gave a pressure higher by 15 and 20 GPa than the Au standards of Heinz and Jeanloz[13] and Jamieson,[8] respectively, at a pressure of 150 GPa. While the extrapolated Jamieson isotherm is expected to be somewhat low, our analysis agrees with the room-temperature isotherm of Heinz and Jeanloz, suggesting that the discrepancy between the Au and Pt pressures is due to errors in the Pt standard. Given the importance of accurate pressure standards, the status of the Pt EOS seems to warrant further investigation.

*Note added in proof.* Recently, another paper[46] applying similar methods was published. Tsuchiya makes no reference to the Hugoniot data, and obtains significantly higher room-temperature pressures than we do.

## ACKNOWLEDGMENTS

We thank J. C. Boettger, J. D. Johnson, E. D. Chisolm, and S. Crockett for helpful discussions. This work was supported by the U.S. Department of Energy under Contract No. W-7405-ENG-36.

[1] M.H. Manghnani and T. Yagi, *Properties of Earth and Planetary Materials at High Pressure and Temperature* (Geophysical Union, Washington, D.C., 1998).
[2] R.G. McQueen, S.P. Marsh, J.W. Taylor, J.N. Fritz, and W.J. Carter, in *High Velocity Impact Phenomena*, edited by R. Kinslow (Academic Press, New York, 1970).
[3] L. Burakovsky, C.W. Greeff, and D.L. Preston, Phys. Rev. B **67**, 094107 (2003).
[4] M. van Thiel, A.S. Kusubov, and A.C. Mitchell, Lawrence Radiation Laboratory, Livermore, CA, Technical Report UCRL-50108, 1967 (unpublished).
[5] *LASL Shock Hugoniot Data*, edited by S.P. Marsh (University of California Press, Berkeley, 1980).
[6] L.V. Al'tshuler, A.A. Bakanova, I.P. Dudoladov, E.A. Dynin, R.F. Trunin, and B.S. Chekin, Zh. Prikl. Mekh. Tekhn. Fiz. **2**, 3 (1981) [J. Appl. Mech. Tech. Phys. **22**, 145 (1981)].
[7] W.J. Nellis, A.C. Mitchell, and D.A. Young, J. Appl. Phys. **93**, 304 (2003).
[8] J.C. Jamieson, J.N. Fritz, and M.H. Manghnani, in *High-Pressure Research in Geophysics*, edited by S. Akimoto and M.H. Manghnani (Center for Academic Publishing, Tokyo, 1982).
[9] H.K. Mao, P.M. Bell, J.W. Shaner, and D.J. Steinberg, J. Appl. Phys. **49**, 3276 (1978).
[10] H.K. Mao, J. Xu, and P.M. Bell, J. Geophys. Res. [Solid Earth Planets] **91**, 4673 (1986).
[11] P.M. Bell, J. Xu, and H.K. Mao, in *Shock Waves in Condensed Matter*, edited by Y.M. Gupta (Plenum, New York, 1986).
[12] Y. Akahama, H. Kawamura, and A.K. Singh, J. Appl. Phys. **92**, 5892 (2002).
[13] D.L. Heinz and R. Jeanloz, J. Appl. Phys. **55**, 885 (1984).
[14] S.-H. Shim, T.S. Duffy, and T. Kenichi, Earth Planet. Sci. Lett. **203**, 729 (2002).
[15] A. Khein, D.J. Singh, and C.J. Umrigar, Phys. Rev. B **51**, 4105 (1995).
[16] J.C. Boettger, Phys. Rev. B **67**, 174107 (2003).
[17] D.C. Wallace, Phys. Rev. E **56**, 1981 (1997).
[18] A.F. Voter and S.P. Chen, Mater. Res. Soc. Symp. Proc. **82**, 175 (1987).
[19] O.L. Anderson, D.G. Isaak, and S. Yamamoto, J. Appl. Phys. **65**, 1534 (1989).
[20] In particular, Anderson, *et al.* (Ref. 19) use the term anharmonicity to refer to any volume dependence of $(\partial P/\partial T)_V$. We impose no *a priori* restrictions on this quantity.
[21] T.H.K. Barron, Philos. Mag. **46**, 720 (1955).
[22] S.P. Rudin, M.D. Jones, C.W. Greeff, and R.C. Albers, Phys. Rev. B **65**, 235114 (2002).

[23] M.J. Graf, I.-K. Jeong, D.L. Starr, and R.J. Heffner, Phys. Rev. B **68**, 064305 (2003).
[24] P. Söderlind, O. Eriksson, J.M. Wills, and A.M. Boring, Phys. Rev. B **48**, 5844 (1993).
[25] P. Blaha, K. Schwarz, and J. Luitz, WIEN97, Vienna University of Technology, 1997. (Improved and updated Unix version of the original copyrighted WIEN code, which was published by P. Blaha, K. Schwarz, P. Sorantin, and S.B. Trickey, Comput. Phys. Commun. **59**, 399 (1990)).
[26] D. Singh, Phys. Rev. B **43**, 6388 (1991).
[27] J.W. Lynn, H.G. Smith, and R.M. Nicklow, Phys. Rev. B **8**, 3493 (1973).
[28] G. Simmons and H. Wang, *Single Crystal Elastic Constants and Calculated Aggregate Properties: a Handbook* (MIT Press, Cambridge, 1971).
[29] T.S. Duffy, G. Shen, D.L. Heinz, J. Shu, Y. Ma, H.-K. Mao, R.J. Hemley, and A.K. Singh, Phys. Rev. B **60**, 15 063 (1999).
[30] T. Tsuchiya and K. Kawamura, J. Chem. Phys. **116**, 2121 (2002).
[31] J. Abdallah, Los Alamos National Laboratory Report No. LA-10244-M (unpublished).
[32] A.V. Bushman, G.I. Kanel', A.L. Ni, and V.E. Fortov, *Intense Dynamic Loading of Condensed Matter* (Taylor and Francis, Washington, 1993).
[33] L. Burakovsky and D.L. Preston, cond-mat/0206160 (unpublished).
[34] Y.S. Touloukian, R.K. Kirby, R.E. Taylor, and P.D. Desai, *Thermal Expansion: Metallic Elements and Alloys* (IFI/Plenum, New York, 1975).
[35] R. Hultgren, P.D. Desai, D.T. Hawkins, M. Gleiser, K.K. Kelley, and D.D. Wagman, *Selected Values of the Thermodynamic Properties of the Elements* (American Society for Metals, Metals Park, OH, 1973).
[36] P.B. Allen, Phys. Rev. B **36**, 2920 (1987).
[37] P. Vinet, J. Ferrante, J.R. Smith, and J.H. Rose, J. Phys. C **19**, L467 (1986); J.C. Boettger and D.C. Wallace, Phys. Rev. B **55**, 2840 (1997).
[38] A.H. Jones, W.M. Isbell, and C.J. Maiden, J. Appl. Phys. **37**, 3493 (1966).
[39] R. Grover, J. Chem. Phys. **55**, 3435 (1971).
[40] D.C. Wallace, Phys. Rev. E **56**, 4179 (1997).
[41] D. Hayes, R.S. Hixson, and R.G. McQueen, in *Shock Compression of Condensed Matter-1999*, edited by M.D. Furnish, L.C. Chabildas, and R.S. Hixson, AIP Conf. Proc. No. 505 (AIP, Melville, NY, 2000).
[42] C.W. Greeff, D.R. Trinkle, and R.C. Albers, J. Appl. Phys. **90**, 2221 (2001).
[43] E.D. Chisolm, S.D. Crockett, and D.C. Wallace, Phys. Rev. B **68**, 104103 (2003).
[44] B.K. Godwal, A. Ng, and L. Dasilva, Phys. Lett. A **144**, 26 (1990).
[45] N.C. Holmes, J.A. Moriarty, G.R. Gathers, and W.J. Nellis, J. Appl. Phys. **66**, 2962 (1989).
[46] T. Tsuchiya, J. Geophys. Res., [Solid Earth] **108**, 2462 (2003).